VIP Chemical Sensors

DOI: 10.1002/ange.201100054

Highly Mobile Palladium Thin Films on an Elastomeric Substrate: Nanogap-Based Hydrogen Gas Sensors**

*Junmin Lee, Wooyoung Shim, Eunyeong Lee, Jin-Seo Noh, and Wooyoung Lee**

The design of chemical sensors for commercial applications needs to be improved to meet the requirement of mass production, yet many current strategies in sensor design are increasingly complicated and less accessible to manufacturers. These designs mostly rely on making nanoscale gaps in a material of interest,[1] which allow enhancements in performance and miniaturization. In hydrogen gas (H_2) sensors, nanoscale gaps in palladium nanowires have been widely used to study sensor mechanisms[2] and to develop reversible gas sensing capabilities, which is an important step forward in rational sensor design.[2–9] However, integrating these nanogaps into a large-scale device has been a significant challenge, and as a consequence, it has been difficult to realize a commercially viable device. Approaches that overcome the problem inherent to scalability have been developed in Pd thin-film H_2 sensors,[10–15] but they suffer from low sensitivity, low speed, and poor reliability.[16] Herein, we present a novel, low cost, scalable, and lithography-free but nanogap-based sensing method. This highly mobile thin film on elastomer (MOTIFE) utilizes crack formation in a Pd (and PdNi) thin film generated by stretching the film on an elastomeric substrate to reliably and reproducibly provide highly sensitive H_2 sensors. Not only do we demonstrate that stretching a Pd (and PdNi) thin film on an elastomer creates uniform nanogaps over large areas, the size of which can be controlled down to 300 nm at 25% strain, but we also show that these structures may be used for a high-performance H_2 sensor.

Nanogaps in Pd are extensively used to effectively detect hydrogen gas (H_2). The first demonstration of this concept was carried out with nanogaps, known as break junctions, in electrochemically synthesized Pd nanowires.[2] It was shown that these nanogaps could be used as a core component to increase the sensitivity, response speed, and selectivity to H_2 gas. In the following years, attempts to increase the sensing capabilities of Pd-based structures through the use of nanogaps have been extensive, and various fabrication routes for making nanogaps have been developed. These include 1) bottom-up approaches, in which Pd nanoparticles[17] and nanowires[2,3] are synthesized electrochemically; 2) top-down approaches, in which a single nanotrench on a Pd microwire is formed lithographically;[6–8] and 3) hybrid strategies, in which Pd islands with nanoscale gap separations are grown electrochemically on a lithographically patterned surface.[18] In the context of forming nanogaps, new techniques based on the mechanical breakage of metals in the field of molecular electronics[19] and lithography[20] have also been described. However, none of these approaches are amenable to the fabrication of nanogaps over large areas for practical applications.

Another issue that the break junctions have suffered is that Pd thin films peel off from the surface after repeated H_2/N_2 cycles.[10,13] This defect originates from high mechanical strain (on the order of several GPa) at the incoherent interface between the Pd and surface (for example SiO_2) during the Pd to PdH_x conversion with its accompanying volume change. To address this problem, a flexible polymer substrate could be used with Pd on top if the substrate was mechanically coupled to the Pd to effectively eliminate the origin of the strain at the interface during cycling.[6,7] Previous studies have shown the possibility that a stretchable form of a solid material supported by an elastomeric substrate accommodates large levels of strain without damaging the solid material.[21] In principle, it would be possible to use a soft support under a metal of interest as a means of creating cracks (or nanogaps) in a metal by stretching the support while simultaneously providing a coherent interface between the metal and support during a volume change that reduces the strain at the interface. Herein, we describe a new method for making nanogaps in Pd and PdNi on an elastomeric substrate over large areas using lithography-free approach where the elastomeric substrate acts as a mobile support for forming nanogaps and for eliminating the strain at the interface during Pd and PdNi volumetric changes. Moreover, the highly mobile thin film supported by an elastomeric substrate described herein enables the detection of lower levels of H_2 concentration compared to other types of on–off sensors based on the Pd expansion mechanism.[2–6]

Poly(dimethylsiloxane) (PDMS) was chosen as an elastomeric substrate because of its 1) compatibility with Pd (no interdiffusion); 2) chemical inertness to H_2; and 3) mechanical flexibility. The PDMS substrate (20 mm wide × 10 mm long × 0.75 mm thick) was prepared according to established literature methods.[22] A Pd film (10 mm wide × 10 mm long × 6–10 nm thick; Figure 1a and Supporting Information, Figure S1) was deposited on the PDMS substrate using ultrahigh-

[*] J. Lee,[+] W. Shim,[++][+] E. Lee, Dr. J.-S. Noh, Prof. W. Lee
Department of Materials Science and Engineering
Yonsei University
262 Seongsanno Seodaemun-gu, Seoul, 120-749 (Korea)
Fax: (+82) 2-312-5375
E-mail: wooyoung@yonsei.ac.kr

[++] Current address: Department of Materials Science and Engineering
Northwestern University
2145 Sheridan Road, Evanston, IL 60208-3113 (USA)

[+] These authors contributed equally to this work.

[**] This work was supported by the Priority Research Centers Program (2010-0028296) and by the Seoul Research and Business Development Program (10816).

Supporting information for this article is available on the WWW under http://dx.doi.org/10.1002/anie.201100054.

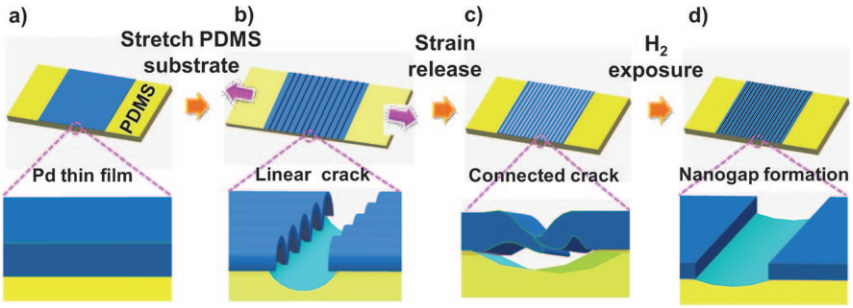

Figure 1. a) Deposition of a Pd thin film on a PDMS substrate using an ultrahigh-vacuum DC magnetron sputter. b) Formation of linear cracks by applying a tensile strain to the PDMS/Pd sample. c) Release of the applied tensile strain. d) Formation of nanogaps in the Pd thin film by utilizing the volumetric change of Pd upon exposure to H_2.

vacuum (UHV) DC magnetron sputtering at a base pressure of 4×10^{-8} Torr. During the Pd sputtering process, the PDMS surface was converted into silica owing to the Ar plasm that easily forms cracks in the PDMS/Pd and increases adhesion between the PDMS and Pd,[23,24] thereby circumventing the need to conduct an additional surface modification. After the Pd deposition, the PDMS/Pd was mounted onto a stretching machine (Supporting Information, Figure S2) and cracks were intentionally generated by stretching the PDMS/Pd sample to a tensile strain of 25% (Figure 1b). The tensile strain in this case is defined as $\varepsilon=[(L-L_0)/L_0]100\,(\%)$, where L_0 is the initial length of PDMS/Pd and L the length of PDMS/Pd in the presence of tensile strain. Depending on the intended use, the width of the cracks (that is, gaps) can be deliberately controlled by the magnitude of the strain applied to the PDMS/Pd. After the tensile strain was released, the PDMS/Pd rebounded to its original position, closing the gaps between the cracked Pd (Figure 1c). To create nanogaps in the Pd film from these closed cracks, we utilized the volumetric change of Pd that occurs after it is exposed to H_2 gas (Figure 1d). This aspect is discussed in further detail below. Finally, for H_2 sensing measurements, the Pd film on the PDMS substrate was electrically connected to a printed circuit board using an Ag paste.

Scanning electron microscopy (SEM) analysis of the resulting cracked Pd thin film confirms that the fabrication method does yield nanogaps in a Pd thin film on a PDMS substrate (Figure 2 and Supporting Information, Figure S3). An applied tensile strain of 25% along the x direction created linear cracks in the y direction perpendicular to the elongation of the 10 nm Pd film on the PDMS substrate. An SEM image showed the cracks had a circa 20 μm center-to-center separation, that the Pd film was broken into pieces through the cracking process (Figure 2a), and the Pd film adhered well to the PDMS surface as a result of the surface modification of the PDMS during the Pd sputtering in an Ar atmosphere. Although most of the cracks were found to have similar width of (2 ± 0.5) μm (Figure 2b), in principle, the crack width can be controlled by the magnitude of the tensile strain applied to the PDMS substrate and the thickness of the Pd film. Furthermore, buckling patterns in the x direction (parallel to the direction of stretching) were observed on the Pd films when the PDMS/Pd was strained (Figure 2a), but these buckling patterns resolved after the stress was released. Note that the cracks and buckling patterns were formed periodically across the 1 cm^2 area simply by stretching the PDMS/Pd (Figure 2c).

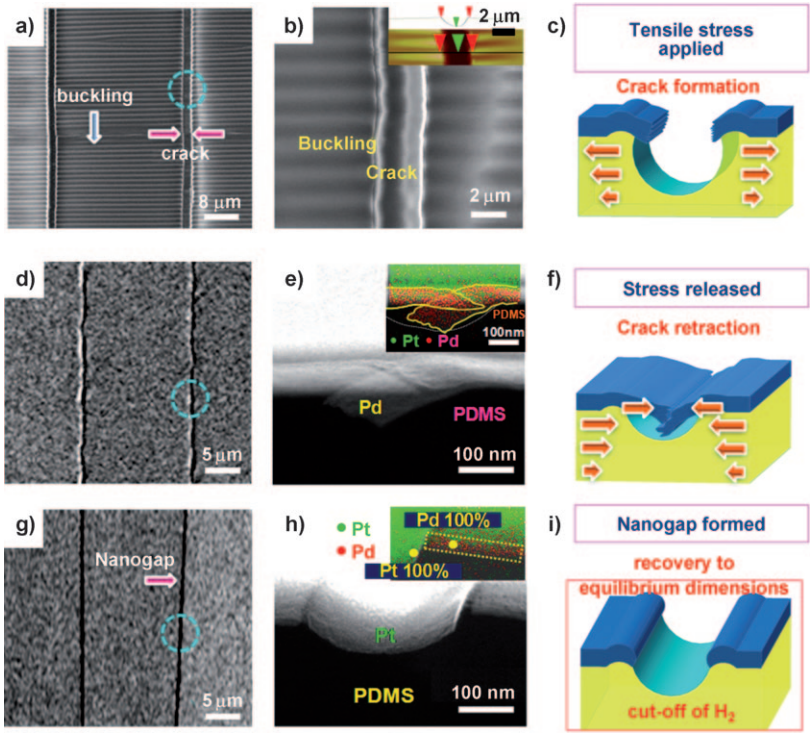

Figure 2. a) A SEM image of a MOTIFE produced by applying a tensile strain of 25% (10 nm thick Pd film used). The directions of cracks and buckling are perpendicular and parallel to the direction of elongation, respectively. b) A magnified SEM image of the crack. Inset: an AFM image of the crack indicating 2 μm wide cracks are formed in PDMS/Pd. c) Illustration of the MOTIFE with 25% tensile strain. d) A SEM image of the MOTIFE after the strain releases. Cracks look less distinct and no buckling patterns are observed. e) A cross-sectional TEM image taken around the crack in the MOTIFE after the tensile strain is released. Elemental mapping for the two ends of the broken Pd film show that they overlap inside PDMS cracks underneath. A Pt layer was deposited for a TEM imaging. f) Illustration of the MOTIFE after the tensile strain is released. g) A SEM image of the MOTIFE after a cycle of exposure to H_2. Nanogaps are shown as black lines on the surface of the Pd film. h) A tilted cross-sectional TEM image of the nanogap. The nanogap formed on a top surface of PDMS (ca. 300 nm wide and 50 nm deep). Elemental mapping over an edge of the crack reveals that Pd elements (pink dots) exist only outside the crack. i) Illustration of the MOTIFE after a nanogap is created using a cycle of exposure to H_2.

After the tensile strain on the PDMS/Pd is released, the cracks are still observable, but they are not as clear as before the strain is released (Figure 2d). On the other hand, the buckling patterns disappear. The average spacing between cracks was about 15 μm. A HR-TEM image of a cross-section of a crack revealed that the broken Pd films overlap inside PDMS cracks underneath (a Pt layer was deposited for a TEM sampling; Figure 2e). As a result, the Pd film on the PDMS is electrically conductive after the strain is released as there is no gap in the cracks. Thus, stretching a PDMS/Pd to 25% and then releasing it results in cracks but no nanogaps on the Pd film (Figure 2f). To create nanogaps, we utilized the mechanism that Pd grains swell upon exposure to H_2, and after the removal of H_2 (insertion of N_2), the grains return to their initial volume but not their initial positions.[2] Indeed, previous studies have shown that this volume contraction creates nanogaps in Pd nanowires.[16,25]

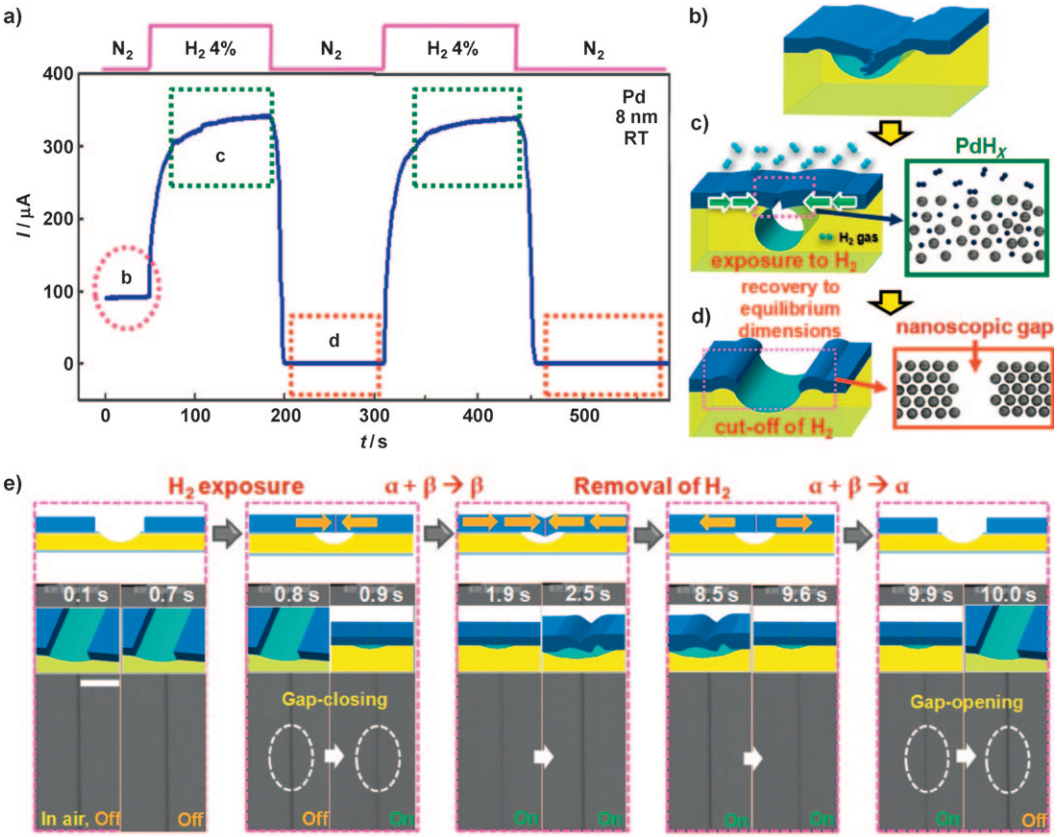

Figure 3. a) The real-time electrical response of a Pd-based MOTIFE to H_2 at room temperature. The hydrogen concentrations are shown in percentages on top of the electrical response. b–d) Illustrations of the on–off operation of the MOTIFE corresponding to the electrical responses shown in (a). e) Optical images taken in a consecutive time series. The corresponding illustrations are shown above the images. Scale bar: 5 μm.

To demonstrate the concept of creating nanogaps, a cracked Pd film on a PDMS substrate was exposed to H_2 converting it into PdH_x, followed by the removal of H_2 gas, the conversion of the PdHx back to Pd, and film contraction. An SEM image subsequently confirmed that the contraction of the overlapped Pd films yields nanogaps (Figure 2g) that are more clearly observable than those before exposure to H_2 (Figure 2d). The gap in the Pd film over the cracked PDMS surface can be seen in a tilted cross-sectional TEM image (Figure 2h). The Pd film was only observed outside the crack on the PDMS substrate (300 nm gap and 50 nm deep). From the elemental mapping analysis (inset of Figure 2h), no Pd is found inside the crack. This is confirmed by EDX data (Supporting Information, Figure S4) that were obtained from outside (spectrum 1) and inside the crack (spectrum 2). The spectra showed that Pd exists only outside the crack, thereby creating a nanogap in the Pd film. This observation indicates that the Pd ends were relocated relative to the PDMS crack owing to the H_2 exposure and subsequent removal (Figure 2i).

In a proof-of-concept demonstration of the H_2 sensing capability of this Pd-based MOTIFE, a nanogapped Pd film on PDMS substrate was put through cycles of H_2 exposure (Figure 3a). The Pd film for the H_2 sensing experiments (8 nm thick) was prepared by the aforementioned procedure (Figure 3b). Provided that the Pd film is exposed to H_2 gas, dissolved hydrogen atoms on the Pd surface penetrate into the Pd film and subsequently increase the interatomic distances, resulting in Pd film swelling on each side the cracks and contact between the ends of the broken Pd pieces (Figure 3c). Saturated current was obtained from an 8 nm thick Pd film exposed to 4% H_2, representing the "on" state (marked with green-dotted boxes in Figure 3a).

The absorbed hydrogen atoms rapidly desorbed upon removal of H_2 gas, resulting in Pd atoms returning to their stable positions with reduced interatomic distances (recovery to equilibrium dimensions; Figure 3d). This hydrogen-desorption process leads to a sudden drop to zero in the current level, namely the "off" state (marked with red-dotted boxes in Figure 3a). More details of gap-closing and opening operation were provided by in situ optical observation (Figure 3e; see also videos in the Supporting Information). The optical images taken in a consecutive time series reveal that the film was mobile upon exposure to H_2, and the

operation was clearly reversible without causing mechanical damage to the film. Note that the images at the time of 2.5–8.5 s show darker contrast at the junction between the two Pd films. This effect is not due to opening of the nanogap, but rather to the Pd films folding downward as they press against each other. The PDMS substrate plays the role of easing the relative lateral motion of broken Pd pieces, transferring a strain in the Pd film to a flexible layer, which synchronizes its motion with that of the Pd film.

The capability that distinguishes the Pd-based MOTIFE H_2 sensor from others in terms of high sensitivity, low detection limit, device reliability, and high response speed (time) was demonstrated (Supporting Information, Table 1), while maintaining the cost advantage of the large-scale thin film process. The H_2 sensing sensitivity, detection limit, and reliability of the Pd-based MOTIFE were evaluated in the context of repeated exposure to H_2 gas of different concentrations, ranging from 0.05% to 10%. A representative electrical response of the Pd-based MOTIFE (10 nm thick Pd, 300 nm gaps in a 1 cm^2 film) to H_2 gas (in an N_2 carrier gas) shows the notable on–off behavior (Figure 4a). The amplitude of the current correlated with the H_2 concentration; a higher concentration results in a greater Pd volume expansion that bridges the gaps, and as a consequence, a larger current crosses the Pd film. When the Pd-based MOTIFE is exposed to a higher H_2 concentration, the nanogaps appear wider after hydrogen desorption because of a greater volume contraction owing to more hydrogen desorption from the PdH_x. For this reason, the detection limit of the Pd-based MOTIFE was 0.4% H_2 after its reaction with 10% H_2, and subsequently the sensor was capable of reversibly sensing up to 10% H_2 over 29 on–off cycles at atmospheric pressure and room temperature. Note that this highly sensitive and perfect on–off sensing over many cycles without the degradation of the Pd film was implemented by forming nanogaps over large areas in a Pd film by stretching a flexible PDMS substrate. In contrast, normal Pd films on hard Si/SiO_2 substrates operate as "normally on", and resistance-based sensors show much lower sensitivity (3.92%, 10 nm Pd film upon exposure to 2% H_2) and shifted baseline resistance (Supporting Information, Figure S5). Furthermore, the response time, defined as the time to reach 90% of the total change in electrical resistance change,[2] was also evaluated. The average response time of the Pd-based MOTIFE was 0.67 s upon exposure to 2% H_2 (Figure 4b), which is fast compared to typical film-type sensors on a hard surface (ca. 64 s, 10 nm Pd films on Si/SiO_2 substrate; Supporting Information, Figure S5). This is due to the facile Pd film movement that opens and closes the gaps upon exposure to H_2, which is assisted by the flexible PDMS substrate.

Finally, the ability to achieve a detection limit below 0.1% H_2 using a different material-based MOTIFE rather than Pd was also evaluated. For example, a sensor using PdNi alloy films was used to suppress the α- to β-phase transition upon exposure to H_2,[12,13,15] and thus quantify electrical signals above 2% H_2, a level at which the Pd-based MOTIFE cannot distinguish (Figure 4a; Supporting Information, Figure S6). A PdNi-based MOTIFE was prepared by the same procedure with the Pd-based MOTIFE (Supporting Information, Figure S7). A representative electrical response of the PdNi-based MOTIFE (6 nm thick PdNi) to H_2 gas (in an N_2 carrier gas) shows the notable on–off behavior with the detection limit of 0.08% H_2 after its reaction with 10% H_2 (Figure 4c). The electrical response above 2% H_2 was easily discernible and accurately quantified H_2 concentrations, and without the rapid phase transition that take places in pure Pd. This different response behavior between the Pd- and PdNi-based MOTIFEs was clearly seen upon exposure to H_2 (Figure 4d), showing that the Pd-based MOTIFE exhibited sudden current change around 1.5% of H_2 owing to the phase transition α to β, while the PdNi-based MOTIFE showed near linear current change. Importantly, the average response time of the PdNi-based MOTIFE upon exposure to 2% H_2 was

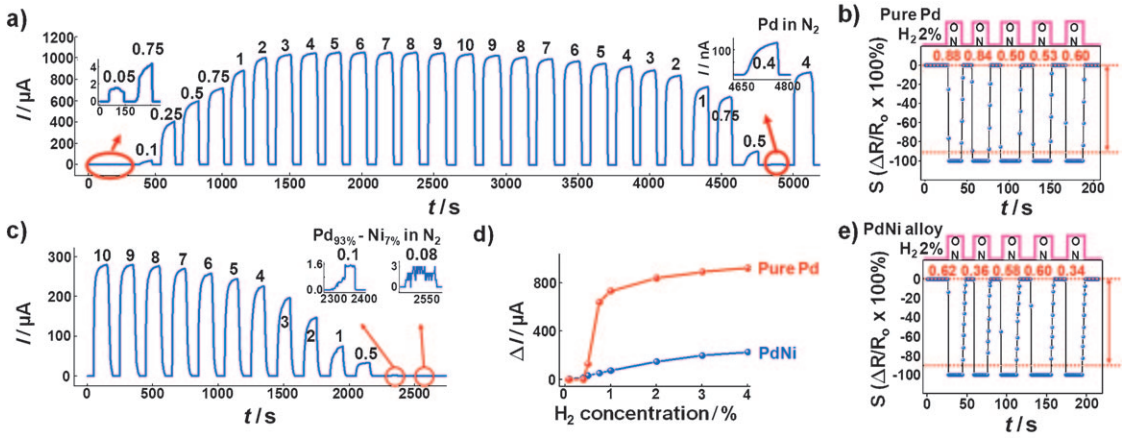

Figure 4. a) The real-time electrical response of a Pd-based MOTIFE to H_2 in N_2 carrier at room temperature. The hydrogen concentrations are shown in percentages on top of the electrical response. b) The sensitivity versus time curve for the Pd-based MOTIFE. The sensitivity was converted from the electrical resistance response. The average response times are 0.67 to 2% H_2 (the time interval between data points is 0.42 s). c) The real-time electrical response of a PdNi-based MOTIFE to H_2 at room temperature. d) The current variation versus H_2 concentration curve for pure Pd-based and PdNi-based MOTIFE during 0–4% H_2. e) A sensitivity versus time curve for the PdNi-based MOTIFE. The average response times are 0.50 to 2% H_2 (the time interval between data points is 0.42 s).

0.50 s (Figure 4e), which is sufficient for commercial applications.

In summary, MOTIFE is a new lithography-free nanogap-based sensing method that uses crack formation over large areas in a metal thin film. Pd- and PdNi-based MOTIFEs can be readily used for highly sensitive and reliable H_2 sensors that show nearly perfect reversible on–off behavior. This novel method is general and can be applied to the creation of nanogaps over large areas on many flat metal surfaces. It is not restricted solely to Pd and PdNi alloys for sensing H_2 because the method is general and can be applied to other metals (see the Supporting Information, Figure S8 for Ti and S9 for Bi) that can utilize nanogaps to specifically sense other chemicals. This new set of capabilities will allow researchers and manufacturers to produce low-cost and scalable sensors that are a step towards the realization of high-volume production.

Received: January 4, 2011
Published online: May 9, 2011

Keywords: chemical sensors · elastomers · hydrogen gas sensors · palladium · thin films

[1] F. Favier, Procedia Chemistry, Proceedings of the Eurosensors XXIII Conference, **2009**, *1*, 746.
[2] F. Favier, E. C. Walter, M. P. Zach, T. Benter, R. M. Penner, *Science* **2001**, *293*, 2227.
[3] E. C. Walter, F. Favier, R. M. Penner, *Anal. Chem.* **2002**, *74*, 1546.
[4] S. Cherevko, N. Kulyk, J. Fu, C. Chung, *Sens. Actuators B* **2009**, *136*, 388.
[5] R. Dasari, F. P. Zamborini, *J. Am. Chem. Soc.* **2008**, *130*, 16138.
[6] T. Kiefer, F. Favier, O. Vazquez-Mena, G. Villanueva, J. Brugger, *Nanotechnology* **2008**, *19*, 125502.
[7] F. Yang, D. Taggart, R. M. Penner, *Small* **2010**, *6*, 1422.
[8] F. Yang, S. Kung, M. Cheng, J. Hemminger, R. M. Penner, *ACS Nano* **2010**, *4*, 5233.
[9] O. Dankert, A. Pundt, *Appl. Phys. Lett.* **2002**, *81*, 1618.
[10] F. A. Lewis, *The Palladium Hydrogen System*, New York, Academic, **1967**.
[11] R. C. Hughes, W. K. Schubert, T. E. Zipperian, J. L. Rodriguez, T. A. Plut, *J. Appl. Phys.* **1987**, *62*, 1074.
[12] R. C. Hughes, W. K. Schubert, *J. Appl. Phys.* **1992**, *71*, 542.
[13] R. C. Hughes, W. K. Schubert, R. Buss, *J. Electrochem. Soc.* **1995**, *142*, 249.
[14] E. Lee, J. M. Lee, J. H. Koo, W. Lee, T. Lee, *Int. J. Hydrogen Energy* **2010**, *35*, 6984.
[15] E. Lee, J. M. Lee, E. Lee, J. Noh, J. H. Joe, B. Jung, W. Lee, *Thin Solid Films* **2010**, *519*, 880.
[16] F. Yang, D. K. Taggart, R. M. Penner, *Nano Lett.* **2009**, *9*, 2177.
[17] F. J. Ibañez, F. P. Zamborini, *Langmuir* **2006**, *22*, 9789.
[18] F. Favier, J. Brugger, J. F. Ranjard, French patent application #0757673, **2007**.
[19] M. A. Reed, C. Zhou, C. J. Muller, T. P. Burgin, J. M. Tour, *Science* **1997**, *278*, 252.
[20] R. Adelung, O. C. Aktas, J. Franc, A. Biswas, R. Kunz, M. Elbahri, J. Kanzow, U. Schürmann F. Faupe, *Nat. Mater.* **2004**, *3*, 375.
[21] D. Kim, J, Ahn, W. M. Choi, H. Kim, T. Kim, J. Song, Y. Y. Huang, Z. Liu, C. Lu, J. A. Rogers, *Science* **2008**, *320*, 507.
[22] D. C. Duffy, J. C. McDonald, O. J. A. Schueller, G. M. Whitesides, *Anal. Chem.* **1998**, *70*, 4974.
[23] M. J. Owen, P. J. Smith, *J. Adhes. Sci. Technol.* **1994**, *8*, 1063.
[24] D. Fuard, T. Tzvetkova-Chevolleau, S. Decossas, P. Tracqui, P. Schiavone, *Microelectron. Eng.* **2008**, *85*, 1289.
[25] V. La Ferrara, B. Alfano, E. Massera, G. D. Francia, *IEEE Trans. Nanotech.* **2008**, *7*, 776.